

POST-TENSIONING THE CONNECTION REGION OF PRECAST POST-TENSIONED BRIDGE GIRDERS FOR CONTINUITY

Mutaz M. M. Taha¹ and Yanmin Jia^{}*

Northeast Forestry University (NEFU), College of Civil Engineering, Harbin, China; mutaztaha1@yahoo.com (M. T.); jianyanmin@nefu.edu.cn (Y. J.)

ABSTRACT

In the study, a precast post-tension concrete girder was tested to examine the behavior of the structure before and after continuity and to evaluate the effectiveness of post-tensioning for continuity to resist positive and negative moments in the connection region. The initial stresses were measured in a concrete bridge constructed using simple support precast post-tension girders that achieved continuity by strengthening the girders through post-tensioning the top of the girders at the connection region. The initial stresses were calculated before and after continuity to examine the effects of continuity on prestress levels. The stresses were calculated at the continuity diaphragm to investigate the effect of post-tensioning on continuity moments. A 3D finite-element model was developed via ANSYS to simulate the performance of the precast post-tension concrete girders. In order to achieve continuity, five forms were compared, and the results indicate that post-tensioning for continuity leads to an increase in the compression stress on the sections. The mid-span stress-strain curve results also show that an increase in the load-carrying capacity for models achieves continuity through post-tensioning. The method used to achieve continuity as described throughout the study presented a stiffer response when compared to that of the other forms of continuity.

KEYWORDS

Bridge, Precast, Post-tension, Continuous girder, Finite-element analysis.

INTRODUCTION

Precast prestressed concrete girders are extensively used to construct bridges. In the 1960s, the concept of building continuous precast prestressed concrete bridges was introduced by constructing girders as simple spans that are continuous through cast-in-place conventionally reinforced concrete joints with continuity diaphragms [1, 2]. The system makes a bridge continuous for live loads and superimposed dead load, i.e., a simple span condition for structural dead load. The advantage includes increasing the life cycle of the bridges and reducing maintenance costs by eliminating joints between spans that are problematic, especially in bridges subject to heavy truck loadings [3, 4].

Prestressed precast concrete girders first have pre-cast simply supported girders, and continuity is then introduced by casting a continuity diaphragm between the girders. The continuity leads to continuity moments, and reinforcements in the diaphragm and the connecting ends of the girders are required to resist these moments and prevent cracks. Extended reinforcement at the bottom of the girders is necessary to resist positive moments that may develop due to time-dependent effects including creep, shrinkage, and thermal effects [5] that cause cracks on the girders or on the diaphragms [6, 7]. Various forms were discussed to resist negative moment

connection and to examine the response of continuity as a result of precast post-tensioned girders [8-10]. In a study, a continuity tendon at the top of the girders was provided to resist negative moments by post-tensioning the top of the girders and by using pre-compression continuity diaphragms to inhibit the cracking of the joints and deck. This reduces the congestion of the extended strand in the continuity diaphragm. Various forms of continuity connections were discussed in several extant studies. Tadros, M.K., et al described a technique to create continuity, and the essence of the technique involved coupling the top strand extensions and then introducing tension in the coupled strands [11]. Sousa, C., et al calculated the prestress level for continuity achieved by placing post-tensioned strands in a cast-in-place deck [12]. Bridge girders achieve continuity via external tendons [13, 14]. Tan, K.H. and R.A. Tjandra created continuity for bridges with partial continuity by using an external tendon [15] and indicated an increase in the load-carrying capacity.

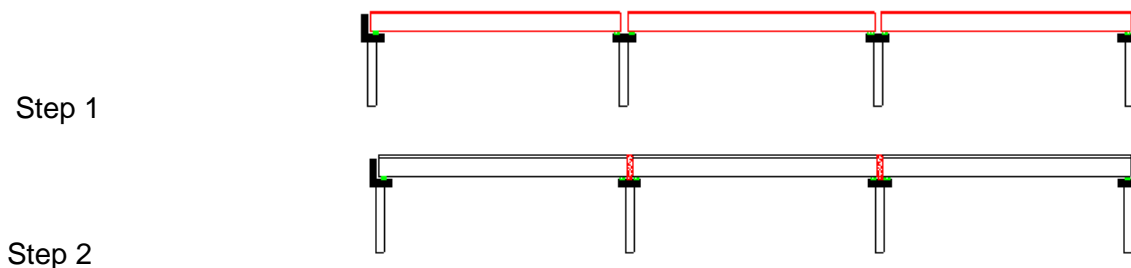
The present study describes a method of post-tensioning for creating continuity, presents a field test and finite-element model of post-tensioned girders, and outlines the stresses on the girders and diaphragm. In order to investigate the efficiency of post-tensioning the top of the girders for continuity, the behavior was compared with various forms of continuity by using a finite-element analysis program (ANSYS).

METHODS

Construction sequence and connection details

The method accomplishes a precast post-tensioned concrete bridge. The method utilizes post-tensioned precast girders; the top of the interior girder ends is post-tensioned to provide continuity prior to casting the deck. The system involves the following steps as shown in Figure 1.

1. Erect post-tensioned precast members with a reinforcement extending beyond member ends at the interior joints.
2. Form, pour, and cure continuity and intermediate diaphragms. It is in contact with the girder ends and the deck above. This is performed to carry the compressive force and the negative moment due to the post-tensioning spans for continuity.
3. Post-tension and anchor the continuity tendons to the girders at a certain distance from the interior ends. Figure 2 shows details of the continuity cable.
4. Form, pour, and cure the continuous deck.
5. Replace the temporary beds over the interior ends of the girder with a bed over the continuity diaphragm.



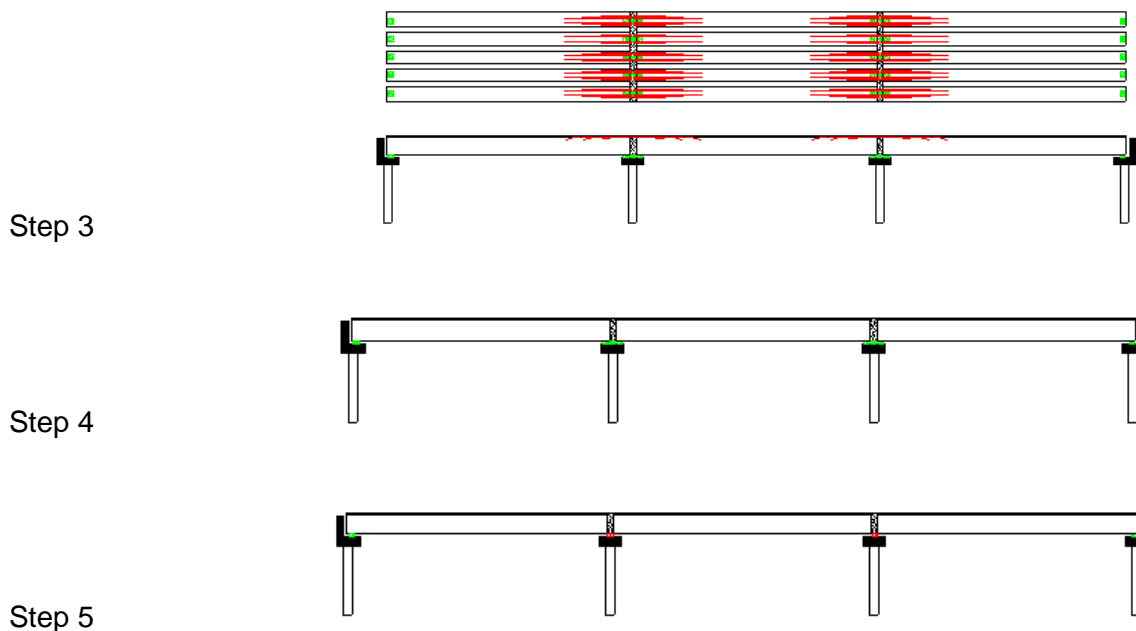


Fig. 1 - Construction sequence of post-tensioning precast post-tension bridge girders for continuity

Bridge description

The bridge consists of three continuous spans (i.e., span 8 corresponding to 39.6 m, span 9 corresponding to 39.2 m, span 10 corresponding to 39.6 m, and continuity diaphragms corresponding to 0.8 m) with a total length of approximately 120 m. The bridge exhibits a width of 12.25 m on five prestressed T girders spaced at 247 cm. The 8-cm RC continuous deck is monolithically cast. The girders exhibit continuity diaphragms with the same cross-section. The intermediate diaphragms have a depth and thickness of 219 cm and 18 cm, respectively. The girders are supported at the continuity connection by a bearing bed at the continuity diaphragms. The bridge elements and dimensions are shown in Figure 2. As shown in Figure 3 (a), the dimensions of the girder are a total height of 250 cm, flange width of 170 cm, and flange thickness of 16 cm. The web thicknesses at the support and mid-span are 60 cm and 20 cm, respectively, and the web thickness gradually decreases along the section as shown in Figures 3(b) and 3(c). The girders were prestressed by using a curved cable profile. Each girder was prestressed for a simple span condition by post-tensioning five cables located at different heights. Specifically, as shown in Figure 3 (a) for the supports and Figure 3 (b) for the mid-span, cable N1 is located at heights of 85 cm and 13.5 cm, cable N2 is located at heights of 123 cm and 13.5 cm, cable N3 is located at heights of 173 cm and 25 cm, and cable N4 is located at heights of 208 cm and 38 cm, at the support and mid-span, respectively. Continuity tendons are anchored on both sides of the girders at a certain distance after pouring the continuity diaphragm is poured, as shown in Figure 4. Cables T1, T2, and T3 are anchored at distances of 1115.7 cm, 810 cm, and 510 cm, respectively, from the support's center, as shown in Figure 4 (a). As shown in Figure 4 (b), the distances of the cross-sections of continuity cables T1, T2, and T3 from the girder's center are 30 cm, 45 cm, and 60 cm, respectively, as shown in Figure 2 (c). Figures 4 (c) and 4 (d) show the details of the continuity cables on the field. The compressive strength of the girders was 34.5 MPa, and the ultimate stress of the seven-wire strand was 1860 MPa.

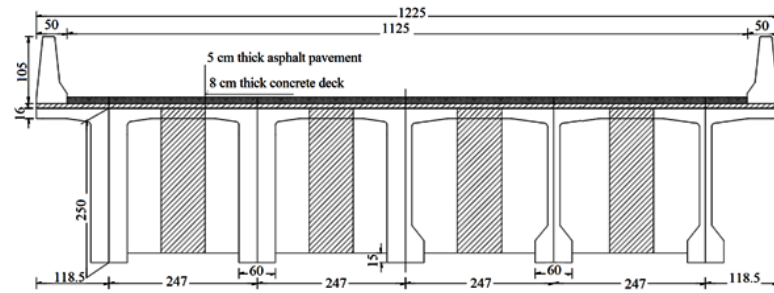
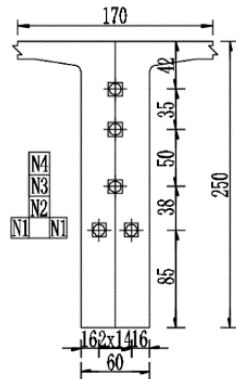
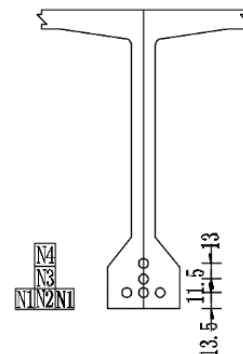


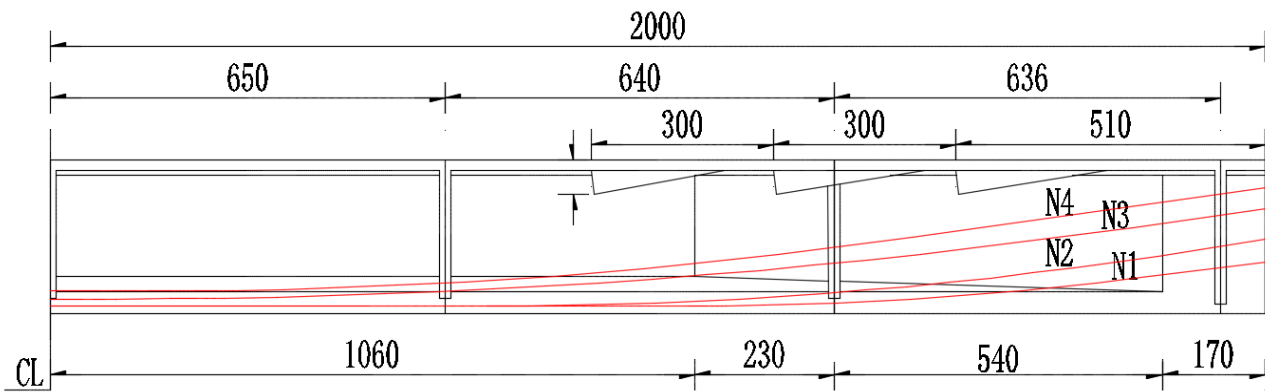
Fig. 2 - bridge dimension



(a) Cross section at support

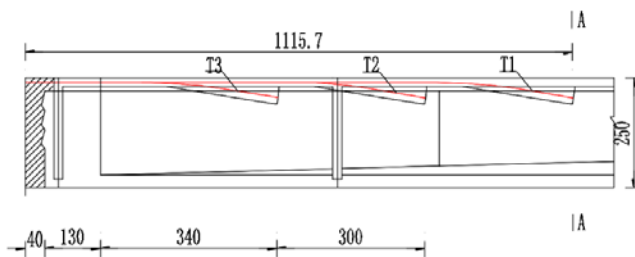


(b) Cross section at mid-span

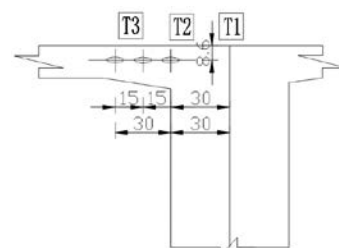


(c) Longitudinal dimension

Fig. 3 - Girder dimension and cable profile



(a) Continuity cable anchorage



(b) Cross-section details

Fig. 4 - continuity cable and anchorage details all dimension in cm.



(c) Anchorage details on the field



(d) Continuity cables top view

Fig. 4 - continuity cable and anchorage details all dimension in cm.

Test Procedure

In order to evaluate specific details and to provide an actual demonstration for the stress distribution, a field test of the concept with continuous post-tensioned girders was performed at the Baobei bridge. The results were obtained during the construction stages of the girders and connection diaphragm as shown by the strain gage layout in Figure 5. The girders were precast and post-tensioned and simply supported by a seven-wire strand with an ultimate stress of 1860 MPa and a jacking stress of 1395 MPa. The continuity tendons were stressed after the girders were appropriately placed and diaphragms were cast. The continuity tendons corresponded to a seven-wire strand with an ultimate stress of 1860 MPa and a jacking stress of 1395 MPa. The girders form three continuous spans and are denoted as spans 8, 9, and 10. As shown in Figure 5, the strain gages at a distance of 3 m from the left supports are denoted as A1-3 (Figure 5 (a)), those to the mid-span are denoted as B1-4 (Figure 5 (a)), those for the principle stress at a distance of 3 m from the right supports are denoted as C1-9 (Figure 5 (a)), the strain gage which impedes the continuity diaphragm for the longitudinal load is denoted as D1-3, and the transfer load is denoted as E1-6 (Figure 5 (b)). The strain gage at the top flange of the girder is denoted as F1-4 (Figure 5 (c)), and strain gages which are attached at intermediate diaphragms are denoted as G1-5 (Figure 5 (d)). During the test, the strain sensor reading was recorded for each loading stage. Figure 6 (a) shows the strain gage recorder. Figure 6 (b) shows the strain gage impeded in the continuity diaphragm to monitor the connection stresses, Figure 6 (c) shows that the strain gage is attached to the girders, and Figure 6 (d) shows the strain gage is impeded in the girder.

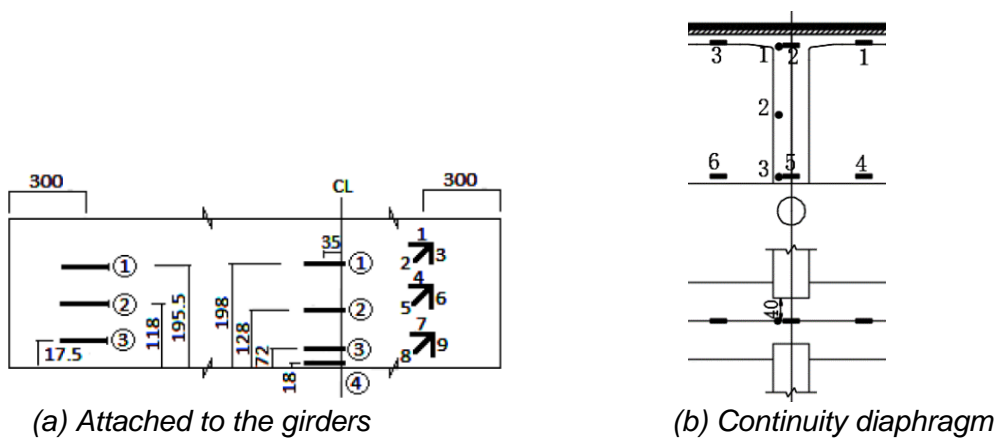


Fig. 5 - strain gage layout

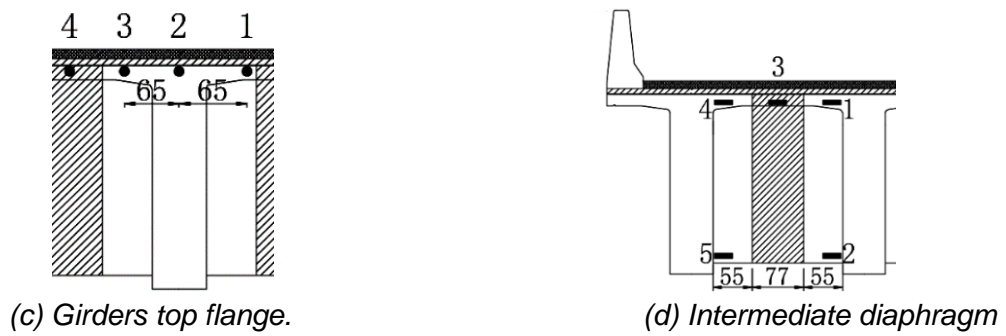
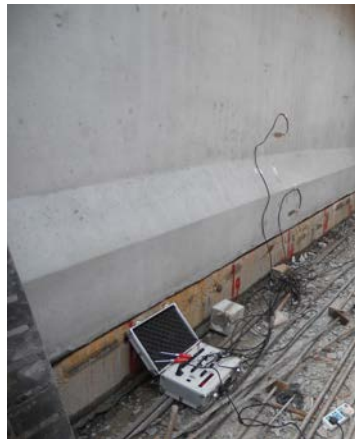


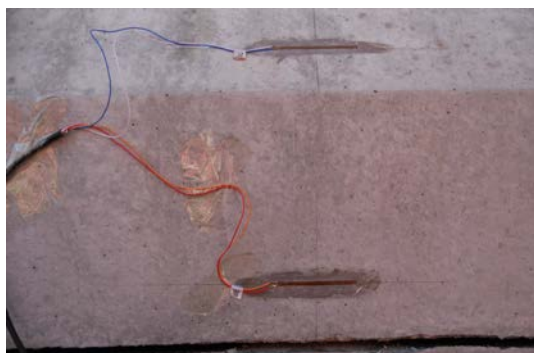
Fig. 5 - strain gage layout



(a) Strain gage recorder



(b) Strain gage impeded in the connection



(c) Strain gage attached to the girders



(d) Strain gage impeded in the girder

Fig. 6 - strain gage during the test and strain gage recorder

RESULTS

During the test, sensor readings were obtained for different strengthening stages. In the simple span conditions, the first reading was taken after strengthening N3 to 50%, reading 2 was taken

after strengthening N2 to 50%, reading 3 was taken after strengthening N1 to 100%, reading 4 was taken after strengthening N2 to 100%, reading 5 was taken after strengthening N2 to 100 %, reading 6 was taken after strengthening N3 to 100%, reading 7 was taken after strengthening N4 to 100%, and the last sensor reading was taken after stabilization. In the continuous conditions, the first cable that was tensioned was T3 left followed by T3 right; second cable that was tensioned was T2 left followed by T2 right; last cable that was tensioned was T1 left followed by T1 right.

Figure 7 shows an example of the strain gage reading of stresses on span 8 and span 9 in the simple span condition. Figure 8 depicts the girder stresses of a continuity condition on span 8 and span 9. Figure 9 illustrates the results of stresses on the continuity diaphragm.

Figure 7 (a) shows the stress corresponding to the readings of strain gages A1 and A2, and shows compression stresses at a distance of 3 m from the support ends. Figure 7 (b) shows compression stresses close to the mid-span at the section where the stresses near the bottom flange are higher. Figures 7 (c) and (d) show the results of principle stress at a distance of 3 m from the right support end. The results correspond to compression stress on the X-component and XY-component, and the vertical stresses on the girder (Y-component) correspond to tension stresses.

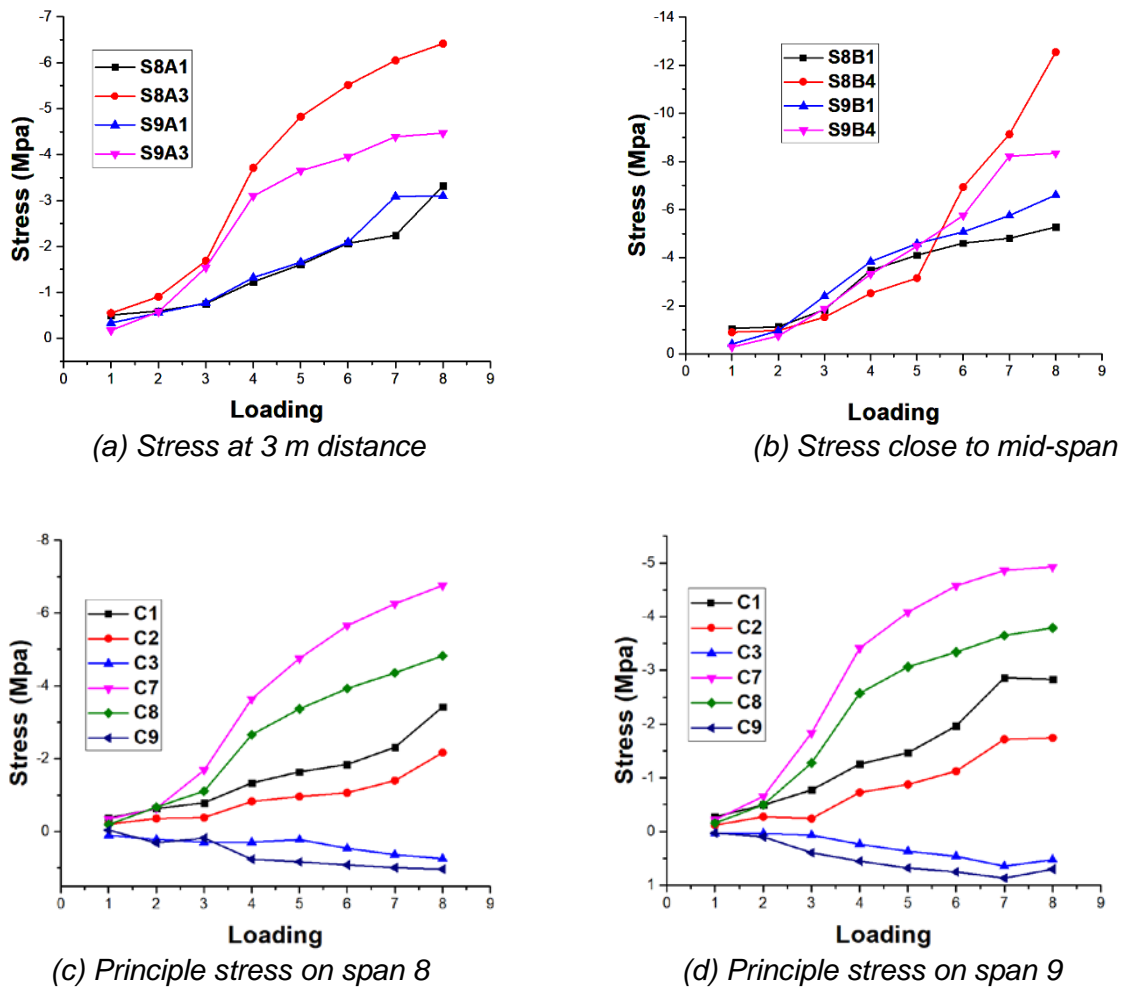
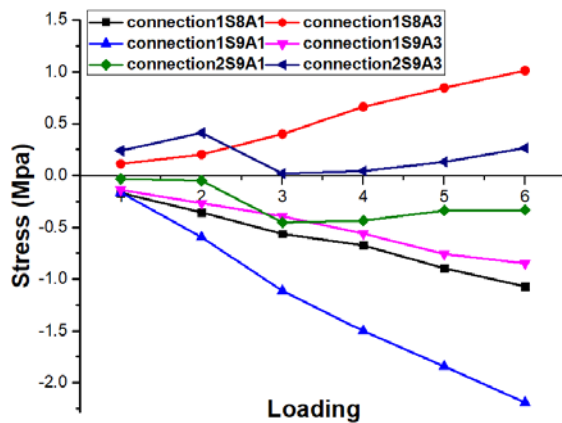
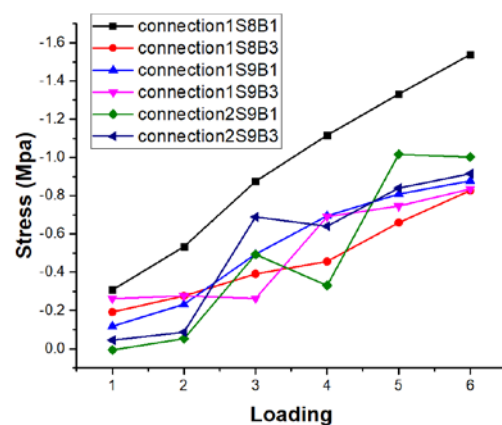


Fig. 7 - Stresses on span 8 and span 9 for simple support condition

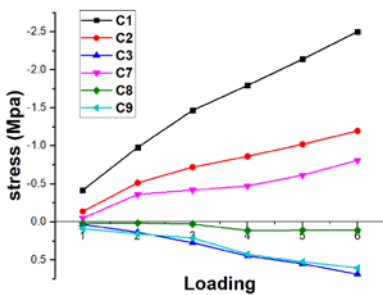
As shown in Figure 8, stresses correspond to the measurements of the strain gages with respect to strengthening of the girders for continuity. Additionally, the stresses on span 9 were recorded at the connection of span 8 with span 9 (connection 1) and at the connection of span 9 with span 10 (connection 2). Figure 8 (a) shows the results at a distance of 3 m from the left support during the post-tensioning of connection 1. Span 8 is subject to compression stress at strain gauge A1 and tension stress at the bottom of the girder. With respect to span 9, the cross-sections of the girders are subject to compression stress due to connection 1 while connection 2 shows tension stresses at the bottom of the girder. Figure 8 (b) shows the stresses close to the mid-span. The results of span 8 and span 9 show compression stresses that increase the prestress level on the girder's cross-section. The stresses on span 9 from strengthening connection 1 and connection 2 exhibit a small difference. Figure 8 (c) shows the principle stresses on span 8, and as expected, the stresses of the X-component correspond to compression while those of the Y-component correspond to tension. Figure 8 (d) shows the principle stress results on span 9 after connecting span 8 with span 9, and the results show compression stresses on the X-component. Figure 8 (e) shows the result of the principle stress on span 9 after connecting span 9 with span 10. The results show compression stress on strain gage C1 and tension stress on strain gage C7; the stress component X-Y corresponds to tension stress.



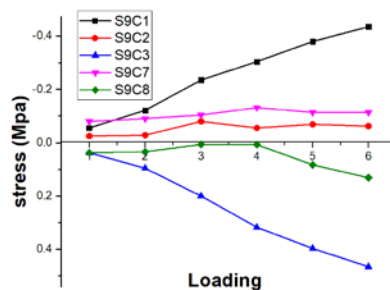
(a) Stress at 3m distance



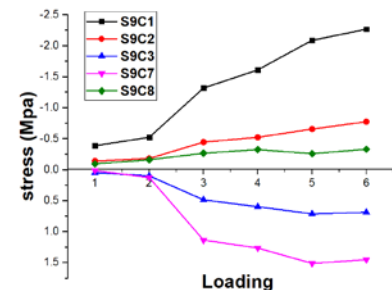
(b) Stress close to mid-span



(c) Principle stress on span 8



(d) Principle stress on span 9



(e) Principle stress on span 9

Fig. 8 - Stresses on span 8 and span 9 of strengthening for continuity

Figure 9 shows stresses corresponding to the measurements of the strain gages on the continuity diaphragms. Specifically, Figure 9 (a) shows longitudinal stresses on the connection

between span 8 and 9, and the results show compression stresses on the continuity diaphragm, which imply that the post-tensioning for continuity resists both negative and positive continuity moments. As shown in Figure 9 (b), the results show the tension transfer stresses.

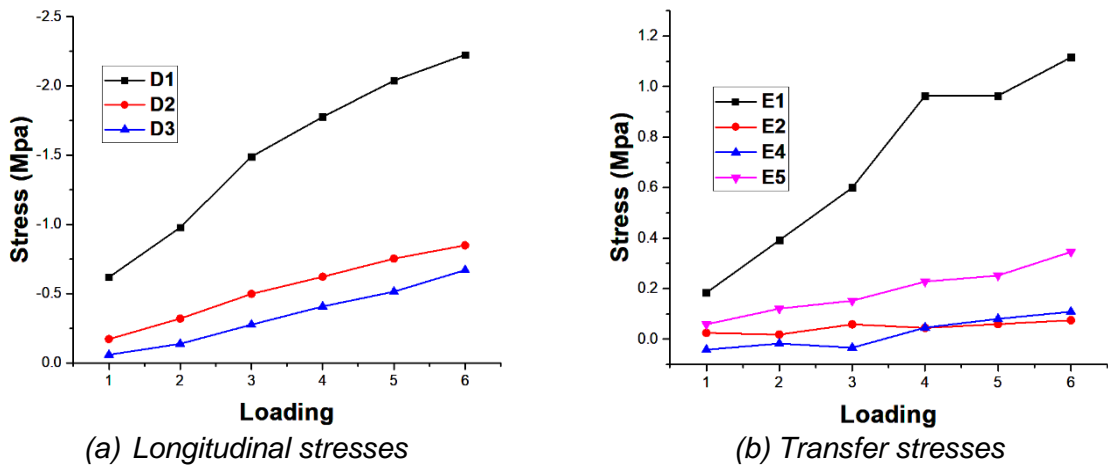


Fig. 9 - Stresses on continuity diaphragm

FINITE ELEMENT ANALYSIS

The finite-element analysis describes a modeling investigation that was conducted to examine the behavior of the continuity of precast post-tensioned beams that were made continuous. An analysis was performed for beams that were made continuous with various connection types to examine the effect of connection methods.

Modelling

In the analysis, five two-span continuous T-beams that were joined by a diaphragm were modeled, in which each beam has a total length of 2950 mm and cross-section dimensions and tendon layouts as shown in Figure 10. The longitudinal reinforcement consisted of two steel bars with a diameter of 16 mm at the bottom and four steel bars with a diameter of 10 mm at the top. Shear reinforcement with a diameter of 6 mm was provided at a spacing of 200 mm. An extended reinforcement bar was provided in the positive moment region for each model. A slab with a thickness of 5 cm with steel bars with a diameter of 12 mm and spacing of 80 mm in the longitudinal direction and 10 mm diameter with a spacing of 200 mm in the transfer direction was connected to the girders and diaphragm. The models were strengthened for a simple span condition with the same tendon configuration including a 7-wire prestressing steel strand with a similar cross-sectional area of 139 mm² per tendon and all tendons were post-tensioned to 950 MPa. The reinforcement yield stress was 540 MPa, the shear reinforcement yield stress was 360 MPa, and the prestressed cables exhibited an ultimate stress of 1860 MPa. The concrete open shear transfer coefficient was 0.5, closed shear transfer coefficient was 1, uniaxial cracking stress was 3, and uniaxial crushing stress was 30. Nonlinear material properties were assumed, equation (1) was used [16] for the nonlinear behavior of concrete, and equation (2) was used [17] for the nonlinear behavior of the 7-wire strand. The stress-strain relation was simulated as multilinear isotropic on ANSYS as follows:

$$\frac{f_c}{f'_c} = \frac{n(\epsilon_c/\epsilon_0)}{n-1+(\epsilon_c/\epsilon_0)^{nk}} \quad (1)$$

$$f_{ps} = \begin{cases} 197,000\epsilon_{ps} & \text{for } \epsilon_{ps} \leq 0.008 \\ 1848 - \frac{0.517}{\epsilon_{ps}-0.0065} < 0.98f_{pu} & \text{for } \epsilon_{ps} > 0.008 \end{cases} \quad (2)$$

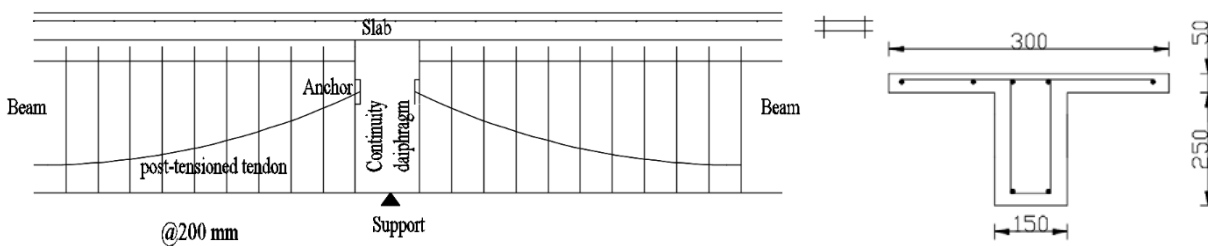


Fig. 10 - model details and cross-section

All models corresponded to a precast post-tensioned condition that achieved continuity. The continuity connections consisted of different combinations, and Figure 11 shows the connection details for each model. Model 1 achieved continuity through a cast-in-place continuous slab. Model 2 achieved continuity through post-tensioning of the end of the girders by post-tensioned prestressed strands as shown in Figure 11 (a). Model 3 achieved continuity through post-tensioned spliced extension strands at the top of the girders as shown in Figure 11 (b). Model 4 achieved continuity through post-tensioning a part of the slab as shown in Figure 11 (c). Model 5 achieved continuity through an external tendon as shown in Figure 11 (d).

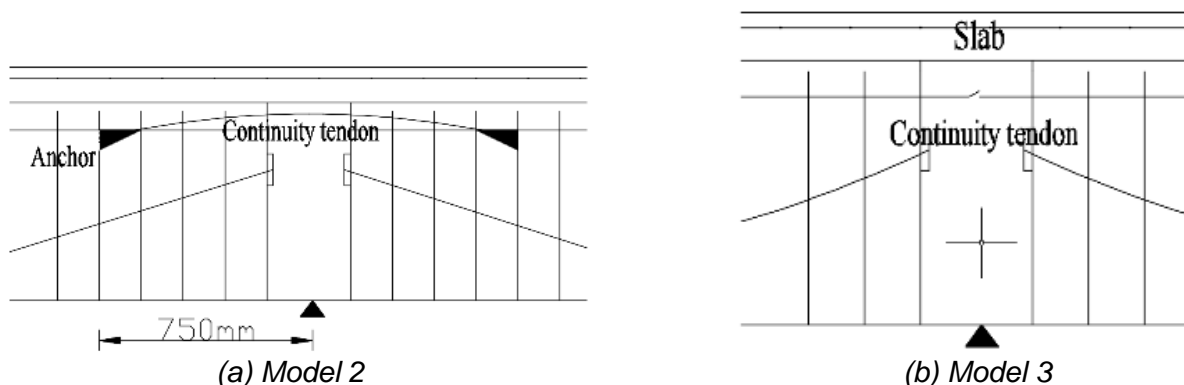


Fig. 11 - Continuity details

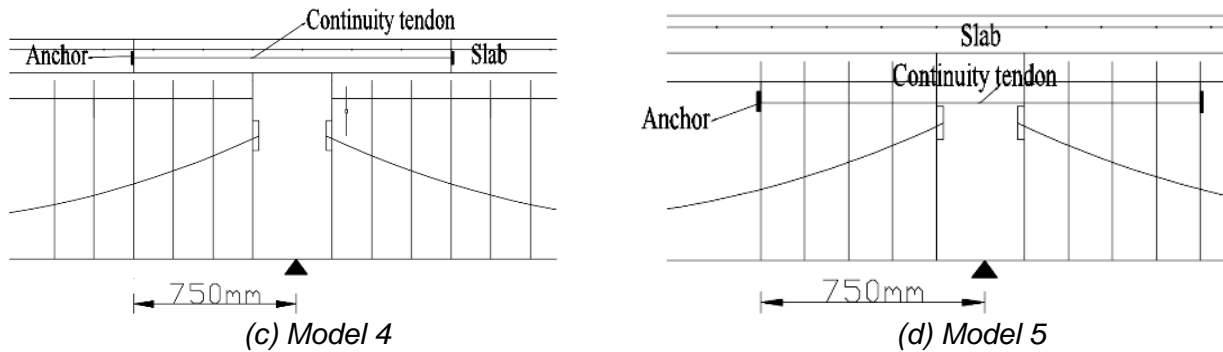


Fig. 11 - Continuity details

Tab. 1 - Material properties

Material	Modulus of elasticity Mpa	Poisson's ratio	Thermal expansion coefficient
Concrete	34500	0.2	-
Prestressing strand	195000	0.3	1.2e-5
Reinforcing Steel	200000	0.3	-

All beams were modeled by using SOLID65 element, and the element includes eight nodes with three translational degrees of freedom at each node. The 3D spar element LINK180 was used to model the prestressing strands and steel reinforcement, and the element exhibits two nodes with three translational degrees of freedom at each node. The SOLID185 element was used to model the anchorage and the supports. Interface between the precast beams and anchorage were bonded to ensure no slip or separation between the two surfaces. The degrees of freedom of the prestressing strands were coupled with the anchorage for all translational and with the girders for vertical translational. Each component was individually meshed to allow the application of the post-tensioning force. The prestressing force was simulated by applying a temperature force. Table 1 shows the material to model the concrete and steel. The FE model of beam 1 is shown in Figure 12, and the final model comprised 10110 elements and 18143 nodes. All models were loaded by 150 KN at the center of each beam.



Fig. 12 - Meshed elements of model 1

Analysis Results

Figures 13 (a) and (b) compare the stress and pre-camber at the bottom of the mid-span due to initial prestressing in beams to achieve continuity with various forms. The maximum pre-camber was 0.32 for model 2. Models 1 and 3 involve the same prestress levels, and the prestress on model 4 exceed that on models 1 and 3.

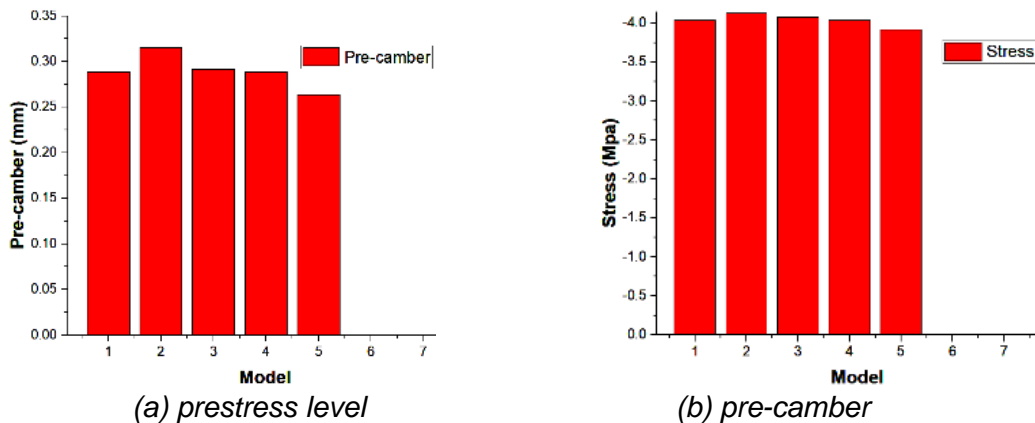


Fig. 13 - stresses and pre-camber due to prestressing force

Figure 14 compares the observed load–deflection characteristics of model 2, model 3, model 4, and model 5 in which all the models were strengthened for continuity with that of the un-strengthened models for continuity, and the deflection of the model was recorded in the section located at the point's load.

The results for models 2, 4, and 5 indicate that strengthening for continuity to a certain distance significantly affects the load deflection response. The deflection of the models increased with the load, and the deflection increments were relatively high for models 1 and 3 before and after cracking. The curve indicated an increase in the load-carrying capacity of models 2, 4, and 5. The capacity increase is attributed to the extension of the continuity tendon to a certain distance. Model 2 revealed that the first cracks occur in the positive moment region at a load of 52 kN and model 2 included first cracks in the positive moment region at a load of 61.5 kN Thus, strengthening the negative moment region resulted in a delay in the cracks in the region. Model 2 exhibited a stiffer response when compared to those of the other models.

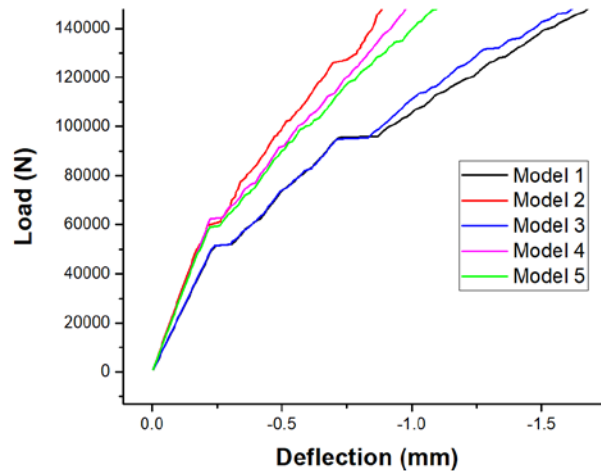


Fig. 14 - stress- strain curve

CONCLUSION

The study describes the method of post-tensioning for continuity. Field tests were conducted on a bridge composed of three-span prestressed concrete girders before and after achieving continuity by outlining the stresses on the girders and diaphragms. A detailed finite-element analysis (ANSYS software) was performed in the study to compare the various forms of continuity. In summary, the following conclusions were obtained:

1. Precast long span concrete girders achieve continuity through the full post-tensioning technique.
2. Post-tensioning precast girders for continuity leads to an increase in the initial compression stresses at the girder sections.
3. Post-tensioning for continuity produces compression in the continuity diaphragm. This results in the resistance of both negative and positive moments in the connection region and elimination of deck cracks and continuity diaphragm cracks.
4. The results of the study indicated a higher initial prestress level and beam stiffness when compared with those of the four different forms of continuity.
5. The results show that the method provided reasonable and conservative estimates of the effect of negative and positive moments.
6. The method exhibited a stiffer response when compared to that of the other forms.

ACKNOWLEDGEMENTS

This research project was sponsored and fully funded by the Inner Mongolia Transportation Department.

REFERENCES

- [1] Kaar, Paul H, Kriz, Ladislav Bohumer and Hognestad, Eivind, 1960. Precast-prestressed concrete bridges: 1. Pilot tests of continuous girders. Portland Cement Association, Research and Development Laboratories, pp. 2 1-37.
- [2] Mattock, Alan H and Kaar, Paul H, 1960. Precast-Prestressed Concrete Bridges: 3. Further Tests of Continuous Girders. Portland Cement Association, Research and Development Laboratories, pp. 5 1-78.
- [3] Thippeswamy, Hemanth K, GangaRao, Hota VS and Franco, Jason M, 2002. Performance evaluation of jointless bridges. *Journal of Bridge Engineering*, vol. 7: 276-289.
- [4] El-Safty, Adel and Okeil, Ayman M., 2008. Extending the service life of bridges using continuous decks. *PCI Journal*, vol. 53: 96-111.
- [5] Miller, Richard A, Castrodale, R, Mirmiran, A and Hastak, M, 2004. Connection of simple-span precast concrete girders for continuity. NCHRP Report 519, Transportation Research Board of the National Academies, p. 202.
- [6] Hastak, Makarand, Mirmiran, Amir, Miller, Richard, Shah, Ronak and Castrodale, Reid, 2003. State of practice for positive moment connections in prestressed concrete girders made continuous. *Journal of Bridge Engineering*, vol. 8: 267-272.
- [7] Mirmiran, Amir, Kulkarni, Siddharth, Castrodale, Reid, Miller, Richard and Hastak, Makarand, 2001. Nonlinear continuity analysis of precast, prestressed concrete girders with cast-in-place decks and diaphragms. *PCI Journal*, vol. 46: 60 – 80.
- [8] Hossain, Tanvir, Okeil, Ayman M. and Cai, C. S., 2014. Field test and finite-element modeling of a three-span continuous-girder bridge. *Journal of Performance of Constructed Facilities*, vol. 28: 136-148.
- [9] Eamon, Christopher D., Chehab, Alaa and Parra-Montesinos, Gustavo, 2016. Field Tests of Two Prestressed-Concrete Girder Bridges for Live-Load Distribution and Moment Continuity. *Journal of Bridge Engineering*, vol. 21: p.04015086.
- [10] Ma, Zhongguo, Huo, Xiaoming, Tadros, Maher K and Baishya, Mantu, 1998. Restraint moments in precast/prestressed concrete continuous bridges. *PCI journal*, vol. 43: 40-57.
- [11] Tadros, Maher K, Ficenc, Joseph A, Einea, Amin and Holdsworth, Steve, 1993. A new technique to create continuity in prestressed concrete members. *PCI Journal*, vol. 38: 30-37.
- [12] Sousa, Carlos, Fonseca, Marco, Calcada, Rui and Neves, Afonso Serra, 2013. New methodology for calculation of required prestressing levels in continuous precast bridge decks. *Journal of Bridge Engineering*, vol. 18: 1219-1226.
- [13] Du, J. S., Au, Francis T. K., Chan, Enoch K. H. and Liu, L., 2016. Deflection of unbonded partially prestressed concrete continuous beams. *Engineering Structures*, vol. 118: 89-96.
- [14] Tan, Kiang Hwee, 2014. Beam strengthening by external post-tensioning: Design recommendations. *The IES Journal Part A: Civil & Structural Engineering*, vol. 7: 219-228.
- [15] Tan, Kiang Hwee and Tjandra, Robert A., 2003. Strengthening of precast concrete girder bridges by post-tensioning for continuity. *PCI Journal*, vol. 48: 56-71.
- [16] James K. Wight, James G. MacGregor, 2011. *Reinforced Concrete_ Mechanics and Design* (Prentice Hall) 71 pp.
- [17] Martin, Leslie D Perry, Christopher J, 2004. *PCI design handbook: Precast and prestressed concrete*, chapter 11 (Prestressed Concrete Inst) 32 pp.